Virchows Archiv (1995) 426:281–293

ORIGINAL ARTICLE

Sören Uiker · Wilhelm Kriz

Structural analysis of the formation of glomerular microaneurysms in the Habu venom model

Received: 26 July 1994 / Accepted: 18 November 1994

Abstract The goal of this study has been to characterize the process of glomerular microaneurysm formation and to separate it from capillary ballooning. In the Habu venom model glomerular capillary ballooning and glomerular microaneurysm formation are seen regularly. The sequence of glomerular lesions leading to a glomerular microaneurysm has been examined and it is clear that the process starts with local mesangiolysis. This may proceed to mesangial expansion and/or ballooning of glomerular capillaries but in contrast to ballooning the formation of a glomerular microaneurysm is based on endothelial defects. The process occurs as follows: once initiated by mesangial failure lesions extend along the mesangial axis. As long as the extension of the lesion encroaches on divergent capillary branches, capillary ballooning by "coalescence" is the result. This process comes to an end when convergent capillary branching is reached and two capillaries join. At this point endothelial disruptions occur, blood and mesangial spaces merge and a glomerular microaneurysm is established. Further growth of the microaneurysm occurs following damage spreading along the lobular axis. The entire process has been reconstructed and is presented in a three-dimensional model.

Key words Habu venom · Mesangiolysis · Glomerular capillary ballooning · Glomerular microaneurysm

Introduction

Formation of glomerular microaneurysms in response to the Habu snake venom was first described by Miura and Sumikawa in 1902 [23]. Many other reports have followed [6, 24, 25, 35] and identical or similar lesions have been observed after poisoning with other snake venoms [31, 32, 38] or various chemicals and drugs [1, 14, 42], after temporary glomerular ischaemia [39], systemic hypertension [9, 10, 18], after intravenous injection of anti-Thy 1-1 antibodies [2, 12, 40, 44] and in certain types of glomerulonephritis including diabetic glomerulosclerosis [5, 11, 27, 30, 34, 43].

The mechanism of glomerular microaneurysm formation is not understood. Two-dimensional models of microaneurysm formation [6, 17, 24, 34] characterize this process incompletely. A three-dimensional understanding of the step by step sequence of events of this process, taking into account the branching pattern of glomerular capillaries, is lacking.

It is generally agreed that the failure of the supporting system of the glomerular tuft (mesangiolysis) is the causative underlying damage. It is however unknown how a glomerular microaneurysm develops and why, in most experimental models associated with widespread mesangial damage and in human glomerulopathies, glomerular microaneurysms generally represent a rare event. In the Habu and other venom models, however, microaneurysms are regularly encountered.

Since the mechanism of microaneurysm formation may be assumed to be the same in various glomerulopathies, Habu venom poisoning represents the most convenient model to study this process. We employed high-resolution light microscopy (HRLM), together with transmission (TEM) and scanning electron microscopy (SEM) to elucidate the sequence of events developing into a glomerular microaneurysm.

Material and methods

Twenty-two male Sprague-Dawley rats (Ivanovas, Kissleg, 140–170 g body weight) were divided into six groups of 2–4 animals each, including a control group. The left kidneys were removed after a dorso-lateral incision under pentobarbital anaesthesia (Nembutal, CEVA, 0.12 ml/100 g body weight intraperitoneally). After a recovery period of 24 h lyophilized Habu venom (*Trimeresurus flavoviridis*), dissolved in physiological saline (1 mg/ml), was injected under ether anaesthesia into a tongue vein. A single dose of 3.5 mg venom/kg body weight was given. This procedure was chosen in order to increase the renal effects of the

S. Uiker · W. Kriz (✉)
Institute of Anatomy and Cell Biology I, University of Heidelberg,
Im Neuenheimer Feld 307,
D-69120 Heidelberg, Germany

venom and to minimize mortality [3, 4]. No animal died as a result of the procedure.

After 3, 6, 12, 24 and 32 h between two and four animals and after 18 and 44 h one animal at a time were prepared for in vivo fixation in Nembutal anaesthesia as described previously [13]. Briefly, the abdominal cavity was opened and the abdominal aorta surgically exposed. An aortic segment below the renal arteries – protected by proximal and distal clamps – was cannulated by a polyethylene tube. After fixation of the aortic catheter, the inferior vena cava was opened, the proximal clamp was removed and the perfusion was started. Retrograde perfusion was carried out without prior flushing of the vasculature at a pressure of 230 mmHg for around 2 min at room temperature. The fixative consisted of 1.5% glutaraldehyde and 0.05% picric acid in 0.1 M phosphate buffer (400 mosmol, pH 7.3). Afterwards, the kidneys were removed, divided into pieces, and immersed for at least 12 h in the same solution as used for perfusion. Tissue was processed for TEM, HRLM and SEM.

Small blocks of cortical tissue were weakly osmicated with 0.1% osmium tetroxide in 0.1 M phosphate buffer (pH 7.3) for 1 h. Thereafter the tissue was stained in the dark in a solution containing 1% tannic acid (as a contrast agent) in 0.05 M maleate buffer for 3 h at room temperature, followed by staining in a 1% uranyl acetate solution in the same buffer for another 2 h in the dark at +4° C. This mode of processing is known to preserve extracellular matrices, including microfibrils, and intracellular cytoskeletal elements [36].

Dehydration was carried out in graded series of acetone at temperatures gradually decreasing to −30° C. After dehydration, the temperature was allowed to rise to room temperature and the tissue was embedded in epoxy resin (Epon 812, Serva, Heidelberg) by standard procedures. Semithin sections (around 1 µm) were stained with a mixture of methylene blue and Azure II and were examined with a Polyvar microscope (Reichert-Jung, Nußloch). Ultrathin sections (about 40–90 nm, grey – gold) were stained with uranyl acetate and lead citrate and were examined with a Philips 301 EM.

In addition, tissue from 13 rats including 2 animals in the control group was embedded in paraffin (Paraplast; Monoject Scientific, Ireland) by standard procedures. Sections 3–4 µm thick were cut, stained with haematoxylin and eosin and examined with a Polyvar microscope.

Samples of cortical tissue were prepared for SEM microscopy by osmicating tissue slices 2–3 mm thick for 2 h with 1.5% osmium tetroxide in 0.1 M phosphate buffer followed by dehydration in graded series of alcohol at room temperature. After "critical point drying" with liquid carbon dioxide (Polaron, Watford) the specimens were mounted on aluminum stubs with silver conductive paint. The tissue was sputter-coated with gold (10 nm) and was examined with a Philipscan 500 SEM at 25 kV.

Results

The incidence of glomerular microaneurysms varied from rat to rat. In 5 of 11 experimental animals microaneurysms were rarely found (less than 1% of glomeruli). In the remaining 6 rats the incidence ranged from 2.9%

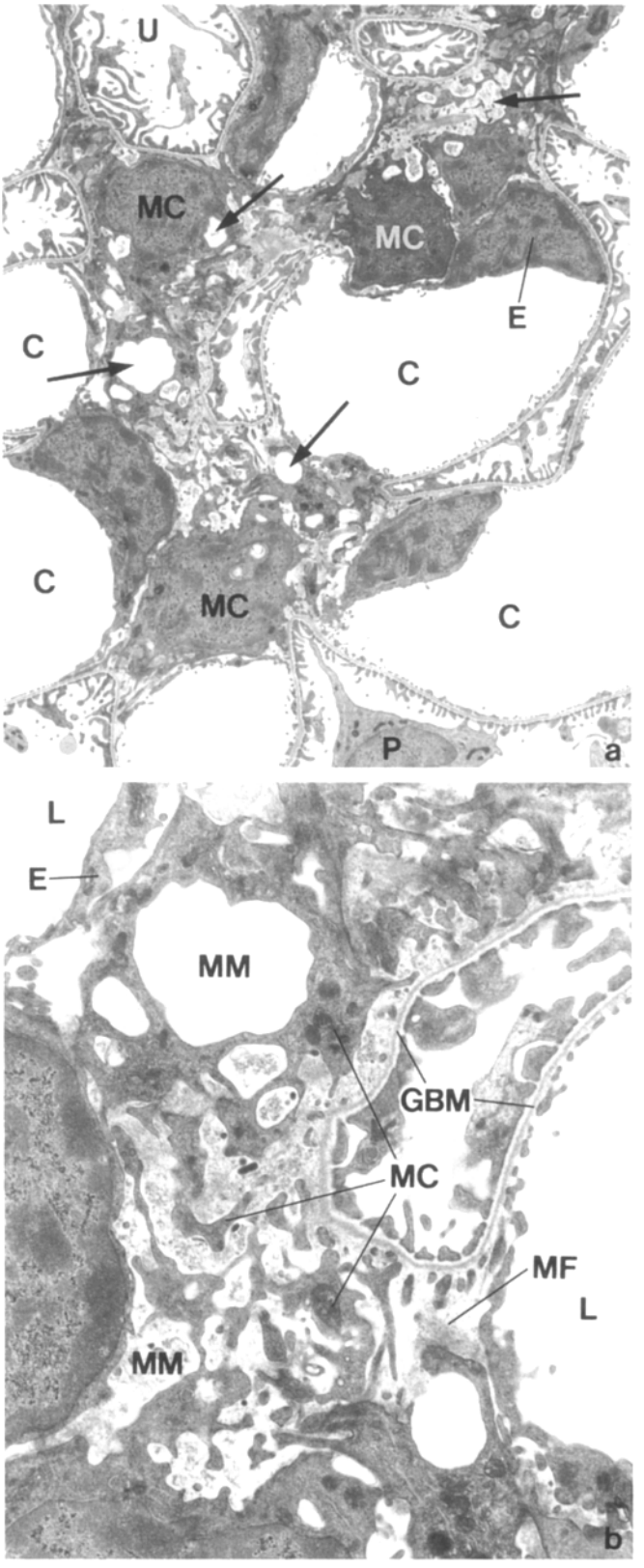

Fig. 1a Overview of an impaired mesangial region with multiple areas of mesangiolysis (*arrows*). Transmission electron micrograph (TEM), ×3200. **b** Enlarged view of the damaged mesangial region shown in (a). Within the matrix anastomosing spaces are seen which appear either empty or contain shreds of matrix material including microfibrils. Mesangial cell (*MC*) processes are arranged in an unstructured pattern, suggesting that they have lost their connections to the glomerular basement membrane (*GBM*). TEM, ×11000. Both 6 h after Habu venom application (*C* capillary, *E* endothelium, *L* lumen, *MF* microfibrils, *MM* mesangial matrix, *P* podocyte, *U* urinary space)

to 30% (mean 15.7%). In all groups a mixture of early and advanced lesions was usually seen. Microaneurysms were found 3 h after venom application; the highest frequency was seen in an animal in the 12 h group. However, early changes (such as local mesangiolysis) were still observed in animals 32 h after drug application.

The lesions appeared to begin with local dissolution of mesangial matrix resulting in disconnections of mesangial cells from the glomerular basement membrane (GBM). As a consequence local expansion of the mesangial spaces, capillary ballooning and finally formation of microaneurysms were seen.

Early changes

The earliest changes consisted of the scattered appearance of electron-lucent spots within the mesangial matrix (Fig. 1a). Those local matrix dissolutions may coalesce to large mesangial areas of decreased electron-density (Fig. 1b) extending frequently into subendothelial spaces. These spaces may contain some material of faint electron-density, frequently granulated in appearance suggesting that they are filled with a proteinaceous fluid. At other places bundles of microfibrils were encountered which had lost any trajectorial pattern but extended in all directions.

Local outpockets of the perimesangial GBM as well as more widespread expansions of the mesangial space were frequently encountered (Fig. 2a). In these areas the usual connections between cells and the GBM were lost. Disconnections of mesangial cells from the GBM at mesangial angles led to widening of subendothelial spaces. This resulted in loss of the typical slim capillary "neck" and eventually in the incorporation of the capillary into the mesangium. Capillary segments were seen which had lost almost any contact with the GBM (Fig. 2b).

Often, mesangial cell profiles appeared to float in the widened fluid filled mesangial spaces. Their processes were short and stubby and were frequently arranged in an unstructured pattern around the cell body (Fig. 1b). Cytologically, the mesangial cells appeared vital, exhibiting an intact cytoskeleton including microtubules and actin filaments. Necrosis of mesangial cells was not seen. The GBM was generally intact. At a few sites splitting into several layers (Fig. 2b) and local thickening were seen.

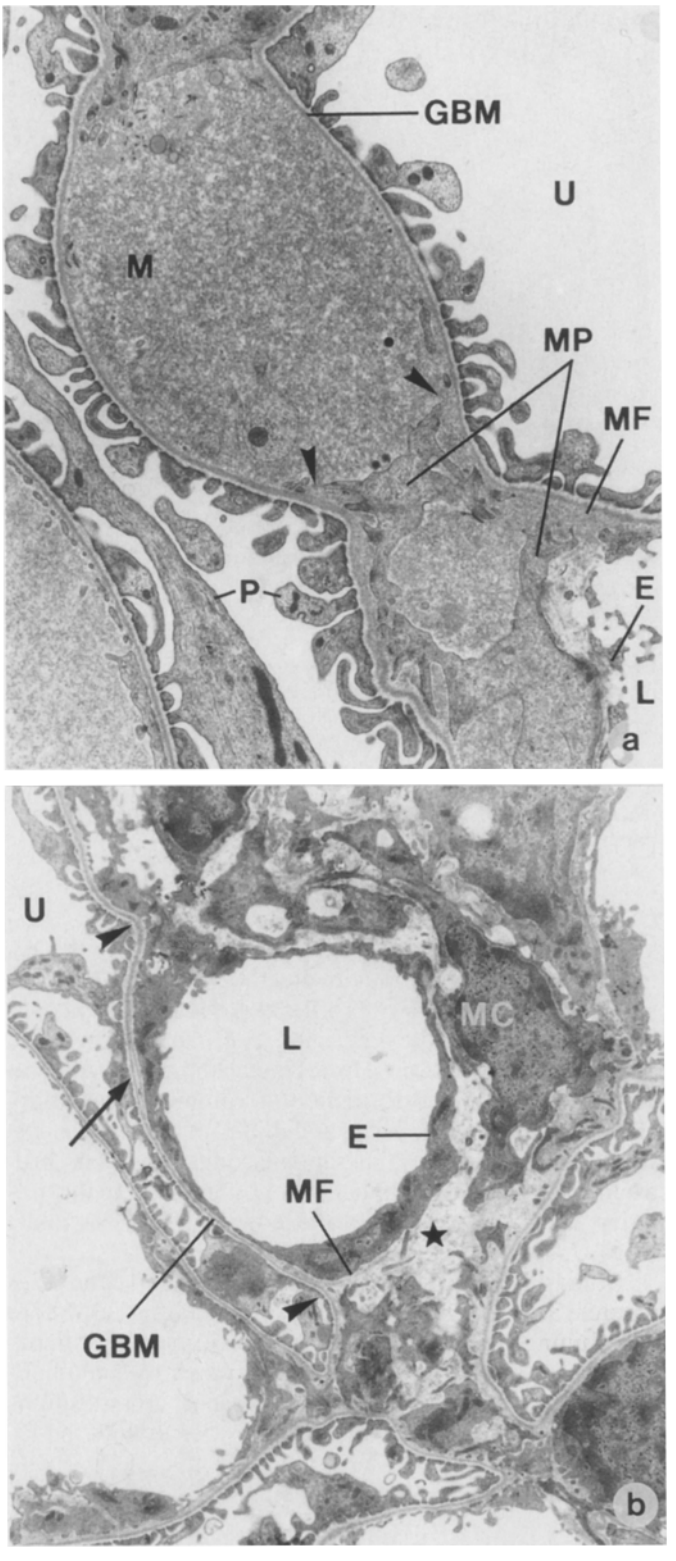

Fig. 2a, b Acute mesangial expansion. **a** Extremely widened mesangial axis bulging into urinary space and filled with amorphous, probably proteinaceous, material. Mesangial cell processes are absent from this area. At sites of intact mesangial cell process – GBM connections opposing parts of the GBM are held together (*arrowheads*). TEM, ×10000. **b** A capillary profile has lost most of its contact to the GBM and is almost fully incorporated into the mesangium. Two depressions in the GBM are seen (*arrowheads*) which probably represent the former mesangial angles of this capillary. The density of mesangial matrix is decreased (*asterisk*). Splitting of the GBM is marked by *arrows*. TEM, ×5100. (**a**) 6 h, (**b**) 3 h after Habu venom application (*MP* mesangial cell process)

Fig. 3 Glomerular profile (probably showing the peripheral part near the tubular origin) with several ballooned capillaries (*1, 2, 3*). Capillary *1* forms a complete ring enclosing an island (*dark star*). The island is a peninsula – see *2* (*arrow*). Note the mesangial agglomeration and protrusion between *2* and *3* (*bright star*). All endothelial and epithelial covers of the ballooned capillaries are intact. TEM, ×1000; 12 h after Habu venom application (*BC* Bowman's capsule)

Capillary ballooning

In addition to the various degrees of mesangial expansion, ballooned capillary profiles were regularly encountered (Figs. 3, 4). Like other models of mesangiolysis [2, 12, 37] loss of widespread mesangial support resulted in capillary dilation and formation of voluminous capillary channels. In general the endothelium of these channels was intact. Frequently, mesangial conglomerations protruding into the vessel lumen were found in dilated capillaries; even at those sites the endothelium was intact (Figs. 3, 4b, c).

Island-like structures inside ballooned capillaries were also seen. They generally consisted of a GBM-core containing an extension of the urinary space accompanied by mesangial remnants and covered by endothelium. Actually, the "islands" represent cross-sections through a "peninsula" which extends deeply into the lumen of a ballooned capillary (Fig. 4a–c).

Glomerular microaneurysms

Glomerular microaneurysms of various sizes were encountered; they may be regarded as the most advanced lesion of the acute phase. In relation to the frequency of large microaneurysms, small and medium-sized ones were surprisingly rare (Fig. 5a–c). This observation suggests that a microaneurysm once formed has a strong

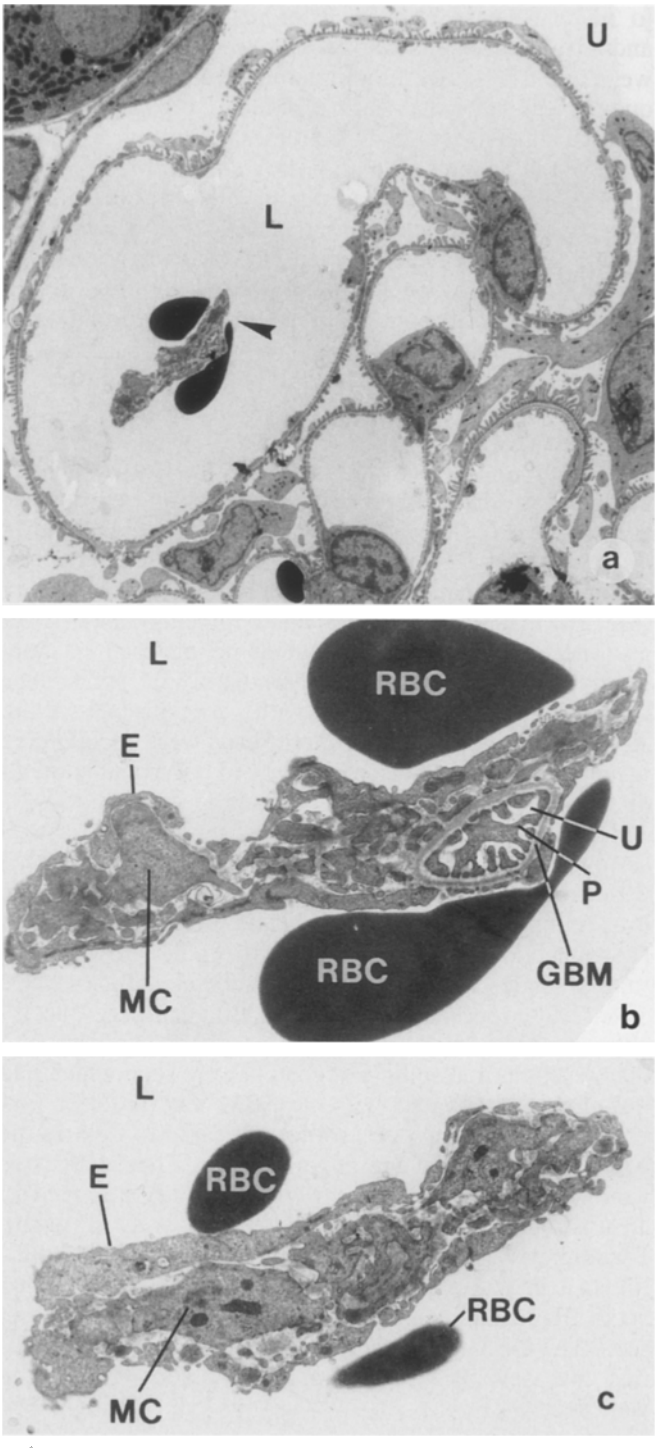

Fig. 4a–c A ballooned capillary with an island in its centre. Seen three-dimensionally this island is a peninsula. **a** Overview (island marked by an *arrowhead*). TEM, ×2000. **b** Enlarged view of the island in (a). It consists of a *GBM* protrusion (note the podocyte foot processes) surrounded by mesangial tissue covered by an intact endothelial layer. TEM, ×8000. **c** The same island from a subsequent section. The *GBM* protrusion has disappeared. The island consists of a mesangial core covered by an intact endothelium. TEM, ×8000; 12 h after Habu venom application (*RBC* red blood cell)

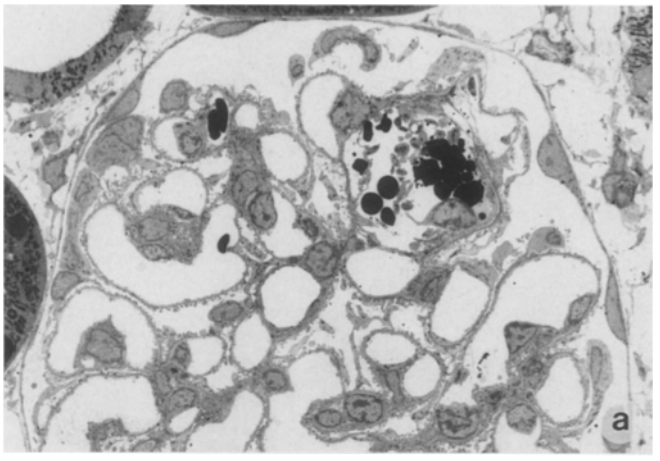

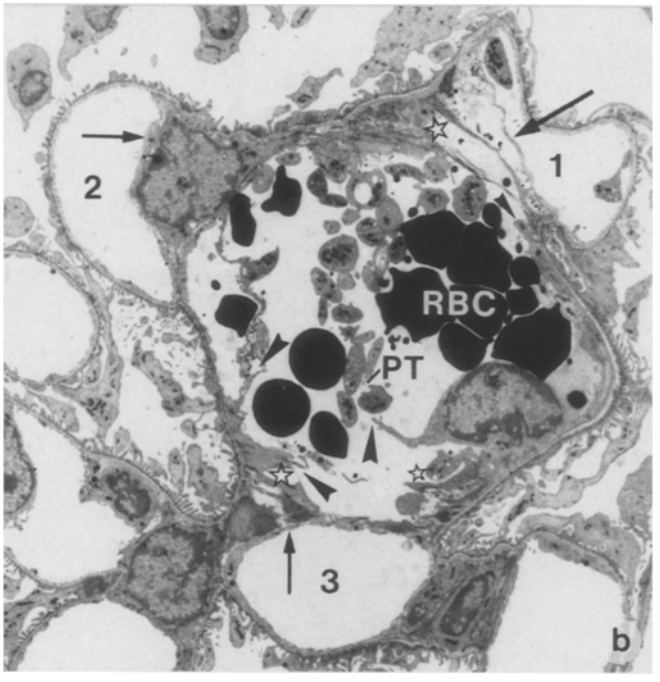

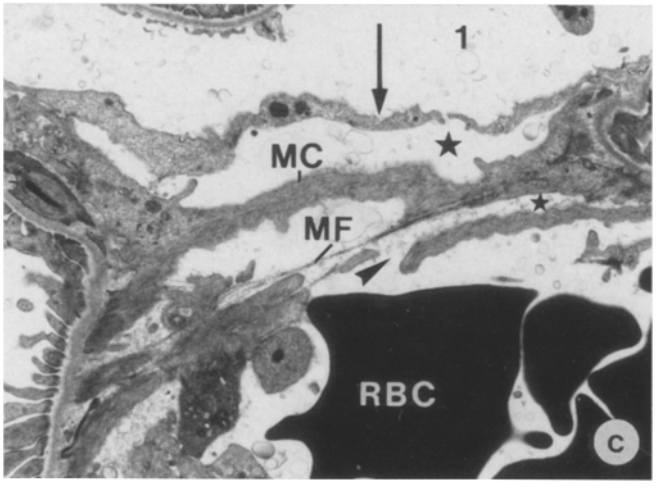

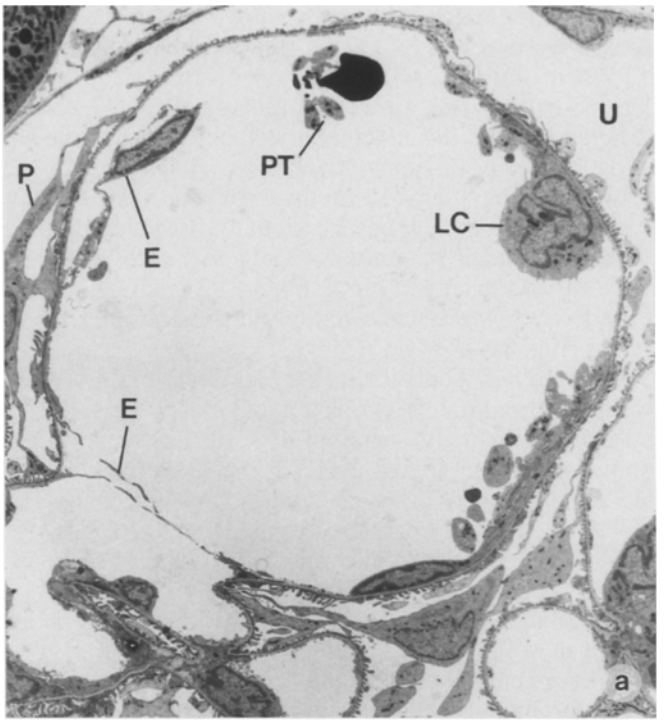

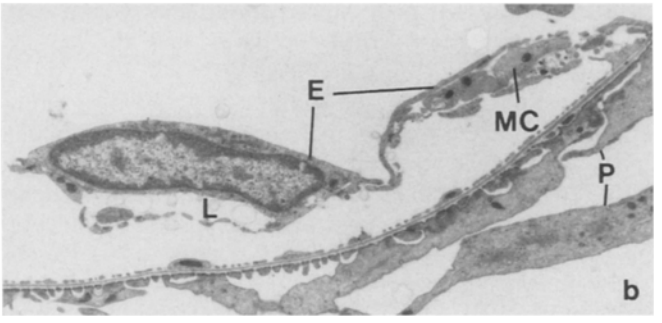

Fig. 6a, b A medium-sized microaneurysm. **a** Overview. The wall of the aneurysm is thin; at its base it is separated from an adjacent capillary only by an impaired endothelial layer. Inside the microaneurysm some platelets and a leucocyte (*LC*) are sticking to the endothelium. On the left side an endothelial remnant is seen protruding into the lumen. TEM, ×2000. **b** Enlarged view of the endothelial protrusion. It can be seen that this protrusion represents a collapsed capillary. The two opposing portions of the endothelium, a slit-like lumen and mesangial remnants are seen. TEM, ×6000. 6 h after venom application

Fig. 5a–c A small microaneurysm. **a** Overview showing the peripheral location of the microaneurysm. TEM, ×800. **b** Enlarged view. In contrast to the surrounding capillaries the microaneurysm is characterized by extensive endothelial damage (*arrowheads*). Its lumen is filled with platelets (*PT*) and erythrocytes. Immediately surrounding the microaneurysm three capillaries are seen (*1, 2, 3*) which appear to be in the process of being incorporated. The interfaces between these capillaries and the aneurysm are stretched out (corresponding to widened capillary necks). The mesangium at these interfaces shows signs of disintegration (*asterisks*); the endothelium lining the capillary lumen is intact (*arrows*). TEM, ×2000. **c** Enlarged view of the interface to capillary *1* (from a subsequent section). Mesangial remnants are seen still interconnecting both mesangial angles. The endothelium of the capillary forms a continuous layer (*arrows*), the endothelium towards the microaneurysm is ruptured (*arrowheads*). The subendothelial spaces are widened (*asterisks*). TEM, ×19500. 6 h after Habu venom application

tendency to enlarge. Multiple aneurysms were extremely rare.

When compared with a ballooned capillary, glomerular microaneurysms were sometimes smaller. The crucial difference lay in the endothelial defect. Generally the endothelium was disrupted over large distances and the capillary lumen merged with the mesangial spaces. Remnants of the endothelium occasionally floated within the vascular channel or were reflected and pressed to the wall of the aneurysm (Fig. 6a, b). Accumulations of thrombocytes were seen even in the smallest microaneurysms (Fig. 5a–c).

Large microaneurysms often had thick, multi-layered walls. In favourable sections it could clearly be seen that a thick wall usually consisted of several alternating endothelial and mesangial layers. The endothelial layer often contained a compressed capillary lumen (Fig. 7a–d).

Enlargement of microaneurysms seemed to follow the axis of a glomerular lobule: one or two lobules often appeared almost unaffected whereas the third was transformed into a huge microaneurysm. SEM revealed an increase in volume of microaneurysmal lobules compared with unaffected ones (Figs. 8a, 11a). These lobules were typically ball-shaped, whereas unaffected lobules appeared compressed and showed a crescent-shaped configuration with mostly oval capillaries near the borderline of two lobules (Figs. 7a, 10a, 11a).

In favourable sections exhibiting the base of a glomerular microaneurysm in the middle part of a lobule, many capillary exits were seen (Fig. 11a). In contrast, only few capillary exits were detected in sections showing an aneurysm with a base near the vascular pole (Fig. 9a–c).

Large, presumably old microaneurysmal lesions were frequently filled with fibrin, red blood cells, polymorphonuclear leucocytes and clusters of platelets (Fig. 10a, b). These aneurysms were mainly seen in the animal group sacrificed 32 h after venom application. Even in those most advanced lesions rupture of the GBM was never noted, but abundant blood cells within Bowman's capsule have been observed repeatedly and may indicate rupture (Fig. 10a).

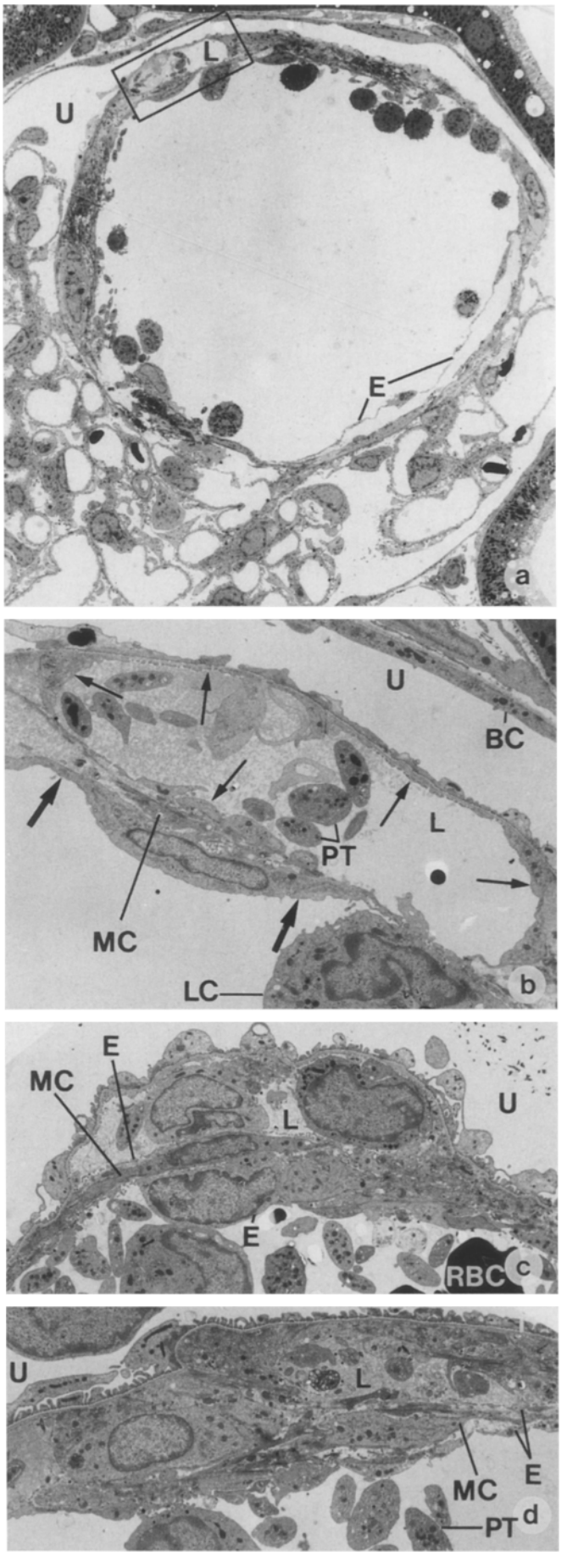

Fig. 7a–d A large glomerular microaneurysm. **a** Overview. In contrast to the microaneurysm shown in Figure 6 the walls of this one are generally thick being composed of several layers. It appears that the multi-layered structure of its wall has developed by the compression of entire capillaries to the microaneurysmal wall. The area designated in (a) is enlarged in (b). TEM, ×720. **b** A partially compressed capillary smoothly opposed to the inner surface of the aneurysm. Note the intact endothelium (capillary endothelium, *thin arrows*; microaneurysmal endothelium, *thick arrows*). TEM, ×3500. **c, d** Multi-layered walls of microaneurysms. In both pictures capillaries appear to be compressed and incorporated into the wall of the microaneurysm [most advanced in (d)]. In addition, at several sites mesangial remnants are seen between the endothelium of the compressed capillary and the inner cover of the microaneurysm establishing a multi-layered microaneurysmal wall. TEMs, (**c**) ×2850; (**d**) ×3750. (**a**) and (**b**) 32 h, (**c**) and (**d**) 12 h after venom application

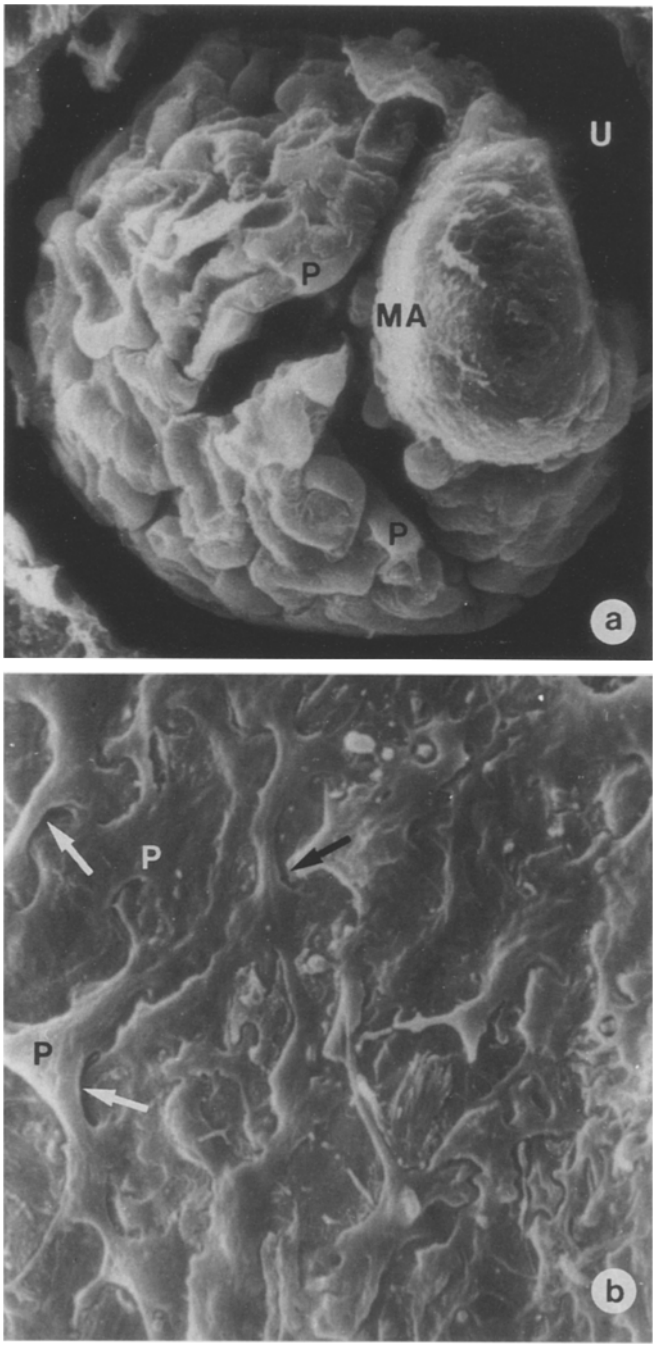

Fig. 8a, b Scanning electron micrographs (SEMs) of the outer aspect of a microaneurysm. **a** A medium-sized microaneurysm is seen protruding out of the globe of the glomerular tuft. Note the borders between individual glomerular lobules. ×1300. **b** Outer surface of a microaneurysm. Podocytes appear extremely stretched out and narrowly opposed to the outer surface. The usual structure of podocytes has totally disappared (*arrows*). ×6250. Both 44 h after Habu venom application; [*MA* microaneurysm]

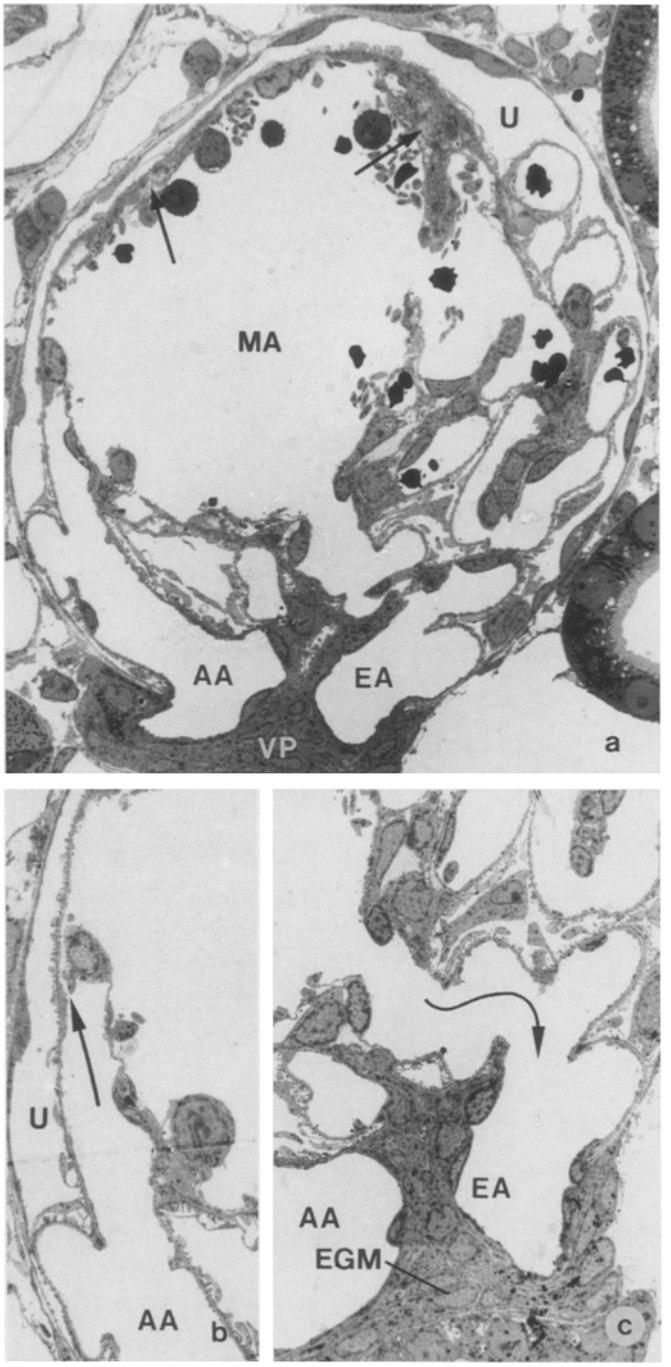

Fig. 9a–c Giant microaneurysm which appears to comprise most of the tuft and attaches to the vascular pole (*VP*). Note that the wall structure varies in thickness comprising thin and thick multilayered parts (*arrows*). Both glomerular arterioles are encountered (*AA* afferent arteriole, *EA* efferent arteriole). TEM, ×760. **b** The connection (*arrow*) of microaneurysm with the *AA*. TEM, ×1400. **c** The connection (*arrow*) of the microaneurysm with the *EA*. TEM, ×1100. All 12 h after Habu venom application; (*EGM* extraglomerular mesangium)

Podocyte lesions

Podocytes overlying ballooned capillaries were frequently flattened and sometimes associated with "pseudocysts" (Fig. 10b). Podocytes covering a large microaneurysm appeared expanded, attenuated and narrowly opposed to the outer capillary surface. At numerous sites the cell bodies or processes seemed to cover the cell bodies and processes of other podocytes (Figs. 8b, 10b). The foot process pattern was extremely simplified. Naked areas of the GBM were also seen.

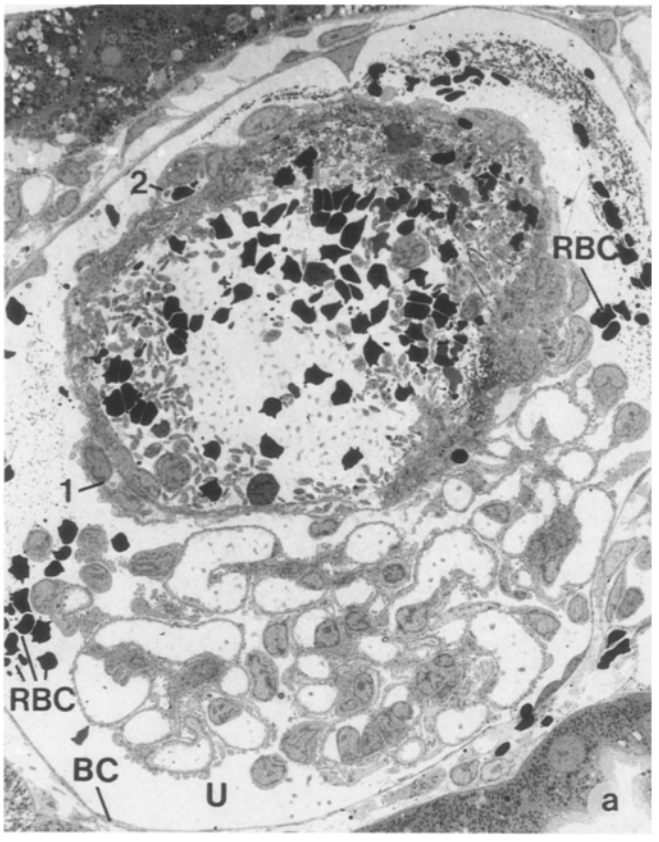

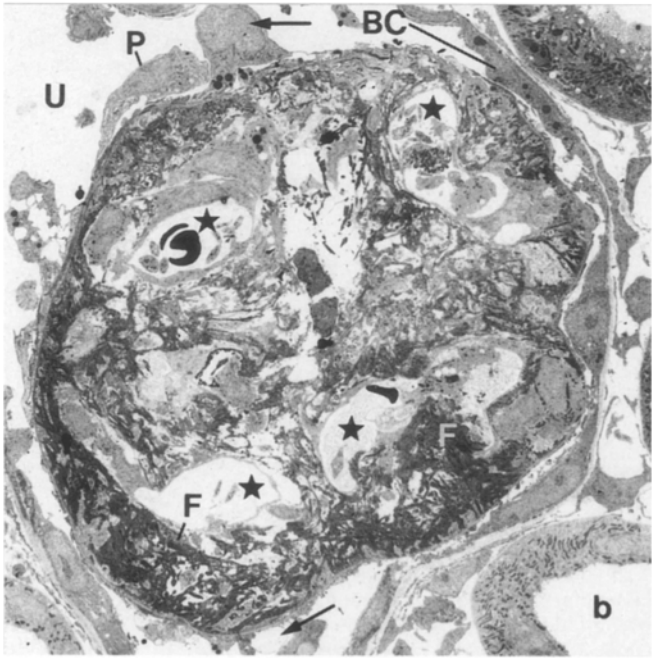

Fig. 10a, b Later stages of microaneurysm development. **a** A large, ball-shaped microaneurysm partially filled with *RBC*, platelets and amorphous material. Blood cells are also seen in the urinary space. The wall of the aneurysm is multi-layered throughout containing several compressed capillaries (*1, 2*). TEM, ×670. **b** Fibrin-filled microaneurysm. Capillary elements (*stars*) are maintained and are included into the agglomerations of fibrin (*F*). Pseudocysts formed by ballooned podocyte processes are marked by *arrows*. TEM, ×1000. (**a**) 12 h and (**b**) 32 h after venom application

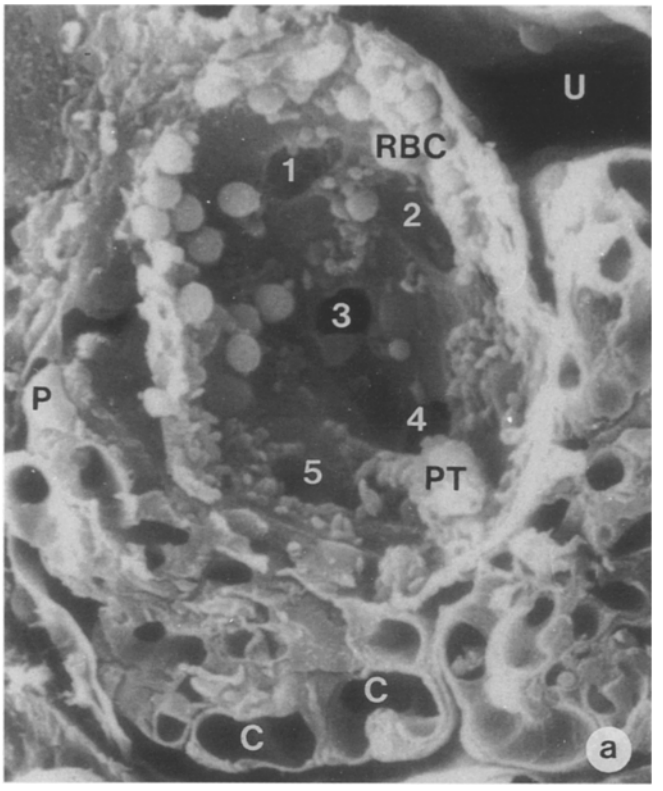

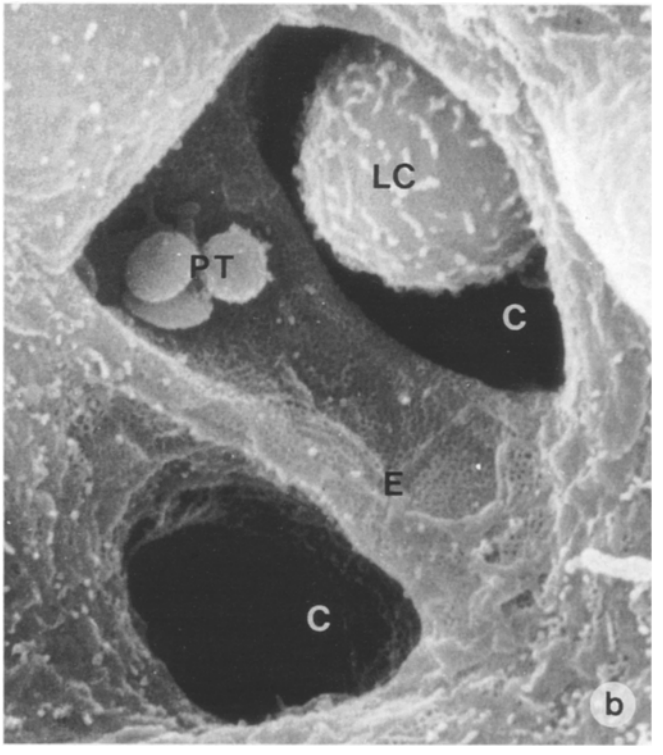

Fig. 11a, b SEM views into the depth of microaneurysms. **a** A whole glomerular profile comprised of three lobules. The middle lobule is transformed into a huge microaneurysm. In the depth of the aneurysmal cavity at least five capillary exits are visible (*1, 2, 3, 4, 5*). Platelets and leucocytes are sticking to the microaneurysmal wall. Note the lobular character of the lesion and the increase in volume of the microaneurysm compared with the intact lobules. ×1500. **b** An enlargement of capillary exits in the depth of a microaneurysm. At this site the endothelium appears intact showing the fenestrated structure. ×10000. Both 44 h after Habu venom application

Discussion

The basic supporting system of a glomerular capillary consists of the GBM and the mesangium [19, 20, 22]. Together, the GBM and the mesangium are considered as a biomechanical unit where the mesangium interconnects opposing parts of the GBM counteracting the distending forces of the blood pressure on the capillary and the perimesangial walls. There are several possible mechanisms of interference with this physiological balance. If the capillary blood pressure rises above a certain level the mesangial cell – GBM connections may burst [39]. As seen in desoxycorticosterone acetate (DOCA) hypertension [9, 18] and in the "one clip – two kidney" model of hypertension [10] sudden, as well as gradual but persistent, rise in capillary pressure may result in disconnections of the GBM from the mesangium. In both models glomerular microaneurysms develop.

However, physiological pressures may lead to capillary ballooning and formation of glomerular microaneurysms if the mesangial integrity is impaired. Since the mesangium consists of the mesangial matrix (providing the connections between the GBM and the mesangial cells) and the mesangial cells themselves (providing the contractile force), damage of either component may result in mesangial failure. Habu venom seems to damage the matrix primarily and exclusively [6, 7]. In contrast, in the anti-Thy 1-1 antibody model of glomerulonephritis the cells are damaged and die [40, 44]. Surprisingly, despite extensive mesangial widening and capillary ballooning in this latter model, formation of microaneurysms is rarely observed (see below).

The sequence of the Habu venom-induced damage starts with local mesangiolysis, followed by mesangial widening, capillary ballooning and the formation of glomerular microaneurysms. The high proteolytic activity of Habu venom appears to be responsible for most of the damaging effects on the glomerular mesangium [14, 38]. This suggestion is confirmed by in vitro observations, such as application of proteinases to isolated glomeruli leading to lobular sacs [16, 17]. In agreement with most authors [6, 7] but in contrast with others [24, 41] we did not observe mesangial cell necrosis. Endothelial damage does occur; Habu venom appears to have a direct toxic effect on endothelium [29]. However, like most other investigators we suggest that most of the endothelial lesions are secondary to the excessive changes in glomerular architecture occurring after destruction of the glomerular skeleton. The same holds true for the GBM. In agreement with previous reports [6, 24] GBM defects in this model are not extensive and do not seem to be important lesions in the progression of damage to a glomerular microaneurysm.

Thus, there is widespread agreement that the primary and crucial damage in the Habu venom model is the dissolution of the mesangial matrix. From a biomechanical point of view this means impairment of the force-transducing extracellular matrices connecting the contractile apparatus of mesangial cells to its effector site the GBM. The inability to develop inwardly directed forces counteracting the outwardly directed distending forces of the blood pressure results in the distention of glomerular structures, starting with the mesangium followed by the capillaries.

Non-Habu venom models of mesangial failure [high pressure models, isolated perfused kidney (IPK), anti-Thy 1-1 glomerulonephritis] do not show consistent formation of glomerular microaneurysms apparently due to their different mechanisms of damage. Although lysis of the mesangial matrix is most probably the main causative factor in the IPK [37], the lack of microaneurysms (despite widespread capillary ballooning) may also be explained by the short duration of the experiments (maximum 2 h). The high pressure models (uninephrectomised-DOCA-hypertension, one clip-two kidneys model [9, 10, 39]) and especially the removal of the clip in the latter model associated with the sudden rise of blood pressure in the formerly clipped kidney are different, since the mesangium may be expected to be intact (or even hypertrophied as has been shown in the DOCA model [18]). The lesions probably result from excessive mechanical load at the mesangium by elevated distending forces. It is easy to accept that the consequences of a failure of the supporting system of the glomerular tuft due to mechanical overload are different from those resulting from a destruction of the supporting system. It is not clear, however, why in the anti-Thy 1-1 model – despite extensive destruction of the mesangium – microaneurysms are comparably a rare event [12, 44].

The differences between both models include the fact that in the Habu venom model the mesangial matrix is destroyed and that in the Thy-1 model it is the mesangial cells which are injured. Moreover, the lesions in the Thy-1 model are widespread, frequently comprising the entire tuft, but lesions in the Habu venom model are generally localized, frequently comprising several areas of the mesangium but never its entirity. The first difference may be responsible for the appearance of the mesangium in the damaged kidney. Mesangial agglomerations developing from a retraction of mesangial cells are never seen in the Thy-1 model; dead cells cannot contract. However, this does not appear to be the crucial difference. We argue that the local character of the damage in the Habu venom model favours the formation of microaneurysms. First, since considerable changes in the haemodynamic conditions at a local nucleus of mesangiolysis are unlikely (capillary pressures at the site of damage in the Habu venom model are probably as high as they are elsewhere in the tuft), an imbalance between the distending forces and the ability of the mesangium to counteract will arise, resulting in local disruption of the supporting system. Second, since the adjacent tuft areas remain intact, the damaged region may expand at the cost of the neighbouring undamaged tissue (which, actually, often appears to be compressed). If – as in the Thy-1 model – the entire mesangium is almost simultaneously destroyed, the effect of such a widespread destruction on haemodynamics is unpredictable (is a high capillary pressure maintained?) and if the mesangium tends to expand at many sites simultaneously the expansions will hinder each other. From this point of view, locally restricted but

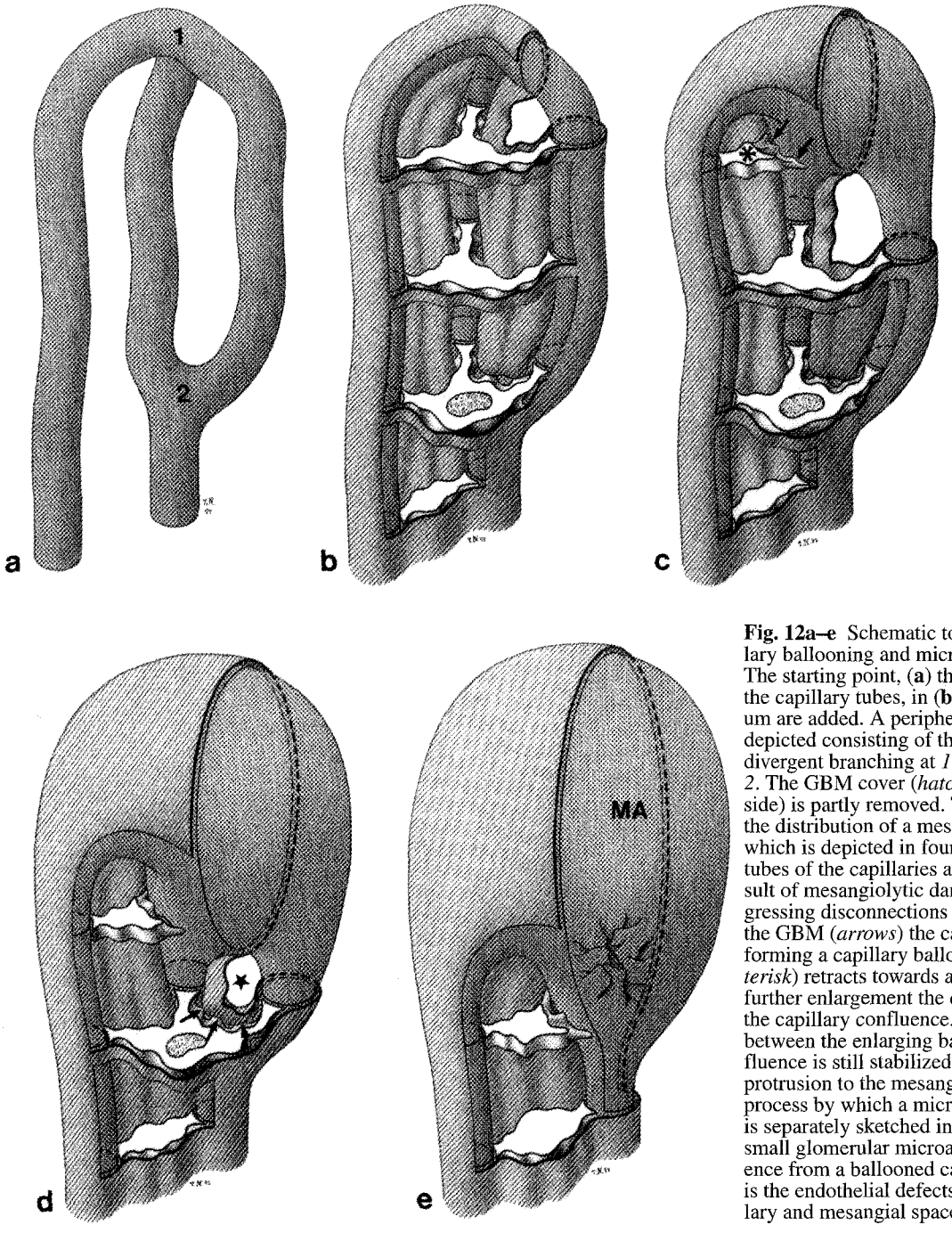

Fig. 12a–e Schematic to show the process of capillary ballooning and microaneurysm formation. **a, b** The starting point, (**a**) the naked branching pattern of the capillary tubes, in (**b**) the GBM and the mesangium are added. A peripheral capillary arrangement is depicted consisting of three capillaries including a divergent branching at *1* and a convergent joining at *2*. The GBM cover (*hatched* on its inner and outer side) is partly removed. The windows allow us to see the distribution of a mesangial cell (*shown in white*) which is depicted in four sections. The endothelial tubes of the capillaries are densely dotted. **c** As a result of mesangiolytic damage going along with progressing disconnections between mesangial cells and the GBM (*arrows*) the capillaries dilate and coalesce forming a capillary balloon. The mesangial cell (*asterisk*) retracts towards a more central position. **d** By further enlargement the capillary balloon approaches the capillary confluence. The remaining gap (*star*) between the enlarging balloon and the capillary confluence is still stabilized by fixations of the GBM protrusion to the mesangium (*arrows*). The crucial process by which a microaneurysm is finally formed is separately sketched in Figure 13. **e** Final stage of a small glomerular microaneurysm (*MA*). The difference from a ballooned capillary (as seen in c and d) is the endothelial defects and the merging of capillary and mesangial spaces (for details see Figure 13)

severe mesangial damage would favour glomerular microaneurysm formation.

The differences in the incidence of glomerular microaneurysms in various models of mesangial failure brings us to the principal question of this study, namely how a microaneurysm develops. The structural analysis has to be made in comparison with capillary ballooning, which is a much more widespread lesion in all these models and which may readily be regarded as the preceding damage to the formation of a microaneurysm.

The process of capillary ballooning has been analysed in detail recently [21, 22, 26]. It has been found that as long as the mesangial damage (the disconnections between mesangial cells and the GBM) spreads along a pattern of divergent capillary branching, the capillaries may simply fuse by coalescence. The mesangium retracts or is moved to more axial portions. This process is sketched in Figure 12a–d. Due to the specific support of glomerular capillaries (the cylinders of the GBM are incomplete) this process allows the fusion of individual capillary loops into a common vascular channel by an unfolding of the GBM. Clearly the endothelium is able to adapt smoothly to the changing surfaces which it lines from inside. Surprisingly, the epithelial cover, the inter-

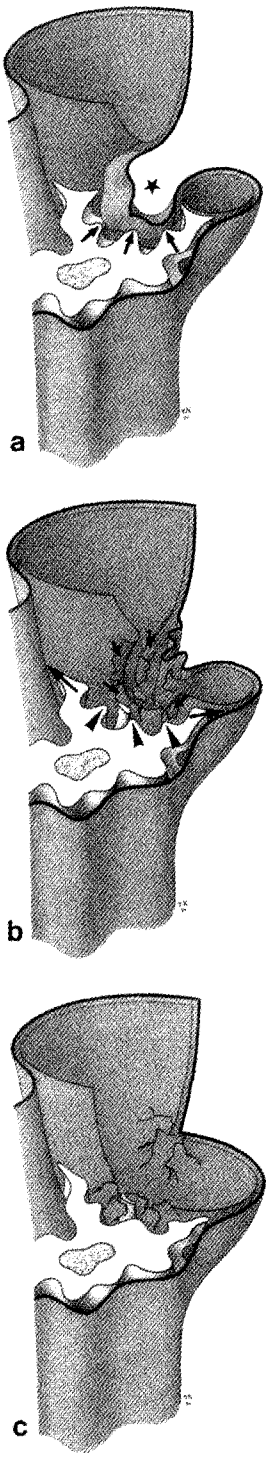

Fig. 13a–c Schematic to show details of microaneurysm formation. **a** An enlargement of the key part of Figure 12d. The gap (*star*) between the enlarging capillary balloon and the capillary confluence is filled by a protrusion of the GBM stabilized by fixations to a mesangial cell (*arrows*). **b** After disconnection of these last fixations the disconnected GBM protrusion slips out of the gap and unfolds. The endothelium at this site loses its support and ruptures (*short arrows*), capillary and mesangial space merge. Mesangial cell processes retract (*arrowheads*). Other mesangial processes do not retract (*long arrows*), becoming interposed between the endothelium and the GBM. **c** General view of the newly formed glomerular microaneurysm. The GBM is entirely unfolded; the wall of the microaneurysm at this site may consist of alternating mesangial and endothelial layers (*arrowheads*)

digitating foot process pattern, is able to follow those extensive changes without disruption. As sketched in Figure 12a–d the retraction of the mesangial cell (after disconnection from its anchoring points at the GBM) allows the unfolding of the basement membrane leading to the gradual ballooning of the capillary loop(s). This appears to be a very common process found in a great variety of glomerulopathies [15, 26]. Even in normal kidneys this process should be regarded as a possible consequence of the specific organization of the structural support of glomerular capillaries. We suggest that ballooned capillaries may be restituted into a normal capillary pattern, as has recently been shown in the anti-Thy 1-1 model of glomerulonephritis [2, 44]. It appears that the glomerular tuft has considerable rebuilding potential but the mechanisms are unknown. Nevertheless, chronic capillary ballooning has considerable pathogenetic relevance in the development of glomerulosclerosis [21, 22].

As soon as the process of mesangial retraction and subsequent capillary ballooning reaches a capillary confluence, the likelihood of ending with irreversible lesions increases dramatically. As can be seen schematically in Figures 12d and 13a, capillary confluence – when seen three-dimensionally – is finally represented by a closed ring of the endothelial tube. Those rings are stabilized by sack-like projections of the GBM extending through the central opening of this ring being fixed at the other side to the mesangium. This stage in the development of a microaneurysm corresponds to the 'islands' encountered frequently in maximally dilated capillary profiles (Figs. 3, 4). If this GBM projection loses its fixation to the mesangium, it will finally slip out of the endothelial ring leaving it unsupported and exposed to unpredictable, possibly abrupt, pressure changes. Due to its shape there is no chance for the endothelium to smooth out (as at divergent capillary branchings). Since the maintenance of a ring structure consisting of a thin endothelial lining without any additional structural support does not seem to be possible, the endothelium ruptures and capillary and mesangial spaces merge (Figs. 12e, 13a–c).

This event marks the point of no return. When compared with a ballooned capillary, another form of damage has come into existence. The process of capillary ballooning does not change the compartmentalization of the tuft: capillary lumina and the mesangium are maintained as separate spaces and the blood flowing through these dilated vessels contacts a normal and continuous endothelium. Disruption of the endothelium changes the situation dramatically. First, the blood does not stay within the vessel, but pours out into the mesangium. Second, contact with the damaged endothelium will obviously trigger thrombotic mechanisms (Fig. 10b). It would be difficult to imagine that such damage could end up with any other consequence than scarring. Actually, it has been shown that the progression to sclerosis is straightforward. Occlusion by a thrombus and organization of this thrombus directly proceeds to sclerosis [9, 26, 33].

Large glomerular microaneurysms are much more frequently encountered than small ones. This suggests that glomerular microaneurysms have a strong tendency to grow; small microaneurysms which represent the beginning of this process, obviously do not stay small for long. We do not know the reason for this. It has become customary to suggest mechanisms following Laplace's law when glomerular capillaries dilate [8, 28]. According to Laplace increasing counterforces (wall tension) are necessary to stabilize a vessel when its radius increases. However, the situation in a glomerular microan-

eurysm is not ideal to argue for Laplace's law. The walls of a microaneurysm are not indefinitely thin; in contrast, the walls may be very thick consisting of several tissue layers (Fig. 7a–d). It appears that the specific organization of the structural support to glomerular capillaries, once seriously damaged, has a tendency to progress along the lobular axis towards the vascular pole. Thereby several mechanisms may contribute to the transformation of a lobule into a single aneurysm. First, mechanisms underlying capillary ballooning and the initial formation of a microaneurysm will go on. In addition, it appears that capillaries running along the periphery of a growing microaneurysm may simply be incorporated into the wall of the microaneurysm by compressing it towards this wall. The multi-layered wall of microaneurysms is frequently seen to consist of alternating layers of mesangium and endothelium. Incompletely compressed capillaries have also been observed leading to the appearance of capillary elements within the aneurysmal wall. The rupture of the endothelium when a microaneurysm is first established appears to be the starting point for a variety of uncontrolled mechanisms progressing inevitably to a fully developed, large microaneurysm reaching the vascular pole of the glomerulus. Whether the process of damage spreading along the axis of a lobule may jump at the vascular pole from one lobule to another is unknown. It is frequently seen that neighbouring lobules are maintained but are compressed by expanding microaneurysms.

In conclusion, the formation of glomerular microaneurysms is seen in a great variety of experimental as well as human glomerulopathies. Generally, they represent a single event whereas the preceding damage, capillary ballooning is a very common glomerular lesion. This study shows that capillary ballooning and formation of a glomerular microaneurysm have to be strictly separated. The step from a ballooned capillary to a microaneurysm occurs at the confluence of two capillaries (convergent capillary branching) and involves the disruption of the endothelium and the merging of capillary and mesangial spaces. Thereby, a new and very serious entity of damage has come into existence which will probably develop into sclerosis.

Acknowledgements The study was supported by Deutsche Forschungsgemeinschaft. The technical assistance of Ms. Hiltraud Hosser and Ms. Brunhilde Hähnel, the photographical work by Ms. Ingrid Ertel and the help of Ms. Marlis Schuchardt in preparing the manuscript are gratefully acknowledged. Special appreciation is given to Rolf Nonnenmacher who did the art work. We also thank Prof. Seiji Sadahiro, National Institute of Health, Tokyo, for providing the Habu venom and Prof. Michio Nagata, Childrens' Hospital, Tokyo University and Prof. Tatsuo Sakai, Juntendo University, Tokyo, for their valuable criticism and cooperation.

References

1. Baehr G (1913) Über experimentelle Glomerulonephritis. Ein Beitrag zur Lehre der Schrumpfniere. Beitr Pathol Anat 55:545–574
2. Bagchus WM, Hoedemaeker PJ, Rozing J, Bakker WW (1986) Glomerulonephritis induced by monoclonal anti-Thy 1.1 antibodies. A sequential histological and ultrastructural study in the rat. Lab Invest 55:680–687
3. Barnes JL (1989) Glomerular localization of platelet secretory proteins in mesangial proliferative lesions induced by Habu snake venom. J Histochem Cytochem 37:1075–1082
4. Barnes JL (1989) Amelioration of Habu venom-induced glomerular lesions: Potential role for platelet secretory proteins. J Lab Clin Med 114:200–206
5. Bloodworth JMB (1978) A re-evaluation of diabetic glomerulosclerosis 50 years after the discovery of insulin. Hum Pathol 9:439–453
6. Cattell V, Bradfield JWB (1977) Focal mesangial proliferative glomerulonephritis in the rat caused by Habu snake venom. A morphological study. Am J Pathol 87:511–524
7. Coffey AK, Karnovsky MJ (1985) Heparin inhibits mesangial cell proliferation in Habu venom-induced glomerular injury. Am J Pathol 120:248–255
8. Daniels BS, Hostetter TH (1990) Adverse effects of growth in the glomerular microcirculation. Am J Physiol 258:F1409–F1416
9. Dworkin LD, Hostetter TH, Rennke HG, Brenner BM (1984) Hemodynamic basis for glomerular injury in rats with desoxycorticosterone-salt hypertension. J Clin Invest 73:1448–1461
10. Helmchen U, Kneissler U (1976) Role of the renin-angiotensin system in renal hypertension. An experimental approach. Curr Top Pathol 61:203–238
11. Hückel R (1938) Eigenartige Glomerulusveränderungen bei benigner Nephrosklerose. Verh Dtsch Ges Pathol 31:392
12. Iversen BM, Kvam FI, Matre K, Morkrid L, Horvei G, Bagchus W, Grond J, Ofstad J (1992) Effect of mesangiolysis on autoregulation of renal blood flow and glomerular filtration rate in rats. Am J Physiol 262:F361–F366
13. Kaissling B, Kriz W (1982) Variability of intercellular spaces between macula densa cells: A transmission electron microscopic study in rabbits and rats. Kidney Int Suppl 22, 12:9–17
14. Kawamura S (1964) Some aspects of mesangial cell proliferation of the renal glomerulus: Correlating factors between mesangial cell proliferation and increased permeability of the glomerular capillary wall. Keio J Med 13:13–41
15. Koitabashi Y, Rosenberg BF, Shapiro H, Bernstein J (1991) Mesangiolysis: an important glomerular lesion in thrombotic microangiopathy. Mod Pathol 4:161–166
16. Krakower CA (1983) The susceptibility of the mesangial matrix of isolated cell-free glomeruli to limited proteolysis. Renal Physiol Biochem 6:250–256
17. Krakower CA, Manaligod JR (1980) Mesangiolysis of isolated renal glomeruli with the formation of lobular sacs or cysts. Renal Physiol Biochem 3:226–236
18. Kretzler M, Koeppen-Hagemann I, Kriz W (1994) Podocyte damage is a critical step in the development of glomerulosclerosis in the uninephrectomised-desoxycorticosterone hypertensive rat. Virchows Arch 425:181–193
19. Kriz W, Elger M, Lemley KV, Sakai T (1990) Mesangial cell-glomerular basement membrane connections counteract glomerular capillary and mesangium expansion. Am J Nephrol 10:4–13
20. Kriz W, Elger M, Lemley KV, Sakai T (1990) Structure of the glomerular mesangium: A biomechanical interpretation. Kidney Int Suppl 38, 30:2–9
21. Kriz W, Hackenthal E, Nobiling R, Sakai T, Elger M (1994) A role for podocytes to counteract capillary wall distension. Kidney Int 45:369–376
22. Lemley KV, Elger M, Koeppen-Hagemann I, Kretzler M, Nagata M, Sakai T, Uiker S, Kriz W (1992) The glomerular mesangium: capillary support function and its failure under experimental conditions. Clin Invest 70:843–856
23. Miura M, Sumikawa T (1902) Beitrag zur Untersuchung des Schlangengiftes. Zentralbl Allg Pathol 13:980–986
24. Morita T, Churg J (1983) Mesangiolysis. Kidney Int 24:1–9
25. Morita T, Kihara I, Oite T, Yamamoto T, Suzuki Y (1978) Mesangiolysis. Sequential ultrastructural study of Habu venom-induced glomerular lesions. Lab Invest 38:94–102

26. Nagata M, Schärer K, Kriz W (1992) Glomerular damage after uninephrectomy in young rats. I. Hypertrophy and distortion of capillary architecture. Kidney Int 42:136–147
27. Nakamoto Y, Takazakura E, Hayakawa H, Kawai K, Dohi K, Fukioka M, Kida H, Hattori N, Takeuchi J (1980) Intrarenal microaneurysms in diabetic nephropathy. Lab Invest 42:433–439
28. Nyengaard JR, Bentsen TF, Gundersen HJG (1988) Stereological estimation of the number of capillaries exemplified by renal glomeruli. APMIS 4:92–99
29. Ohsaka A, Suzuki K, Ohashi M (1975) The spurting of erythrocytes through junctions of the vascular endothelium treated with snake venom. Microvasc Res 10:208–213
30. Olsen S (1974) Extracapillary glomerulonephritis. A semiquantitative light microscopical study of 59 patients. Acta Pathol Microbiol Scand Suppl 82, 249:7–19
31. Pearce RM (1909) An experimental glomerular lesion caused by venom (Crotalus adamanteus). J Exp Med 11:532–540
32. Pearce RM (1913) An experimental study of the late glomerular lesions caused by Crotalus venom. J Exp Med 18:149–155
33. Rennke HG (1988) Glomerular adaptations to renal injury or ablation. Role of capillary hypertension in the pathogenesis of progressive glomerulosclerosis. Blood Purif 6:230–239
34. Saito Y, Kida H, Takeda SI, Yoshimura M, Yokoyama H, Koshino Y, Hattori N (1988) Mesangiolysis in diabetic glomeruli: Its role in the formation of nodular lesions. Kidney Int 34:389–396
35. Sakaguchi H, Kawamura S (1963) Electron microscopic observations of mesangiolysis: The toxic effects of the "Habu snake" venom on the renal glomerulus. Keio J Med 12:99–106
36. Sakai T, Kriz W (1987) The structural relationship between mesangial cells and basement membrane of the renal glomerulus. Anat Embryol (Berl) 176:373–386
37. Sakai T, Lemley KV, Hackenthal E, Nagata M, Nobiling R, Kriz W (1992) Changes in glomerular structure following acute mesangial failure in the isolated perfused kidney. Kidney Int 41:533–541
38. Sakurai N, Sugimoto K, Sugihara H, Shirasawa H, Muro H, Kaneko M, Nikai T, Shibata K (1986) Glomerular injury in mice induced by Agkistrodon venom. Am J Pathol 122:240–251
39. Sheehan HL, Davis JC (1959) Renal ischemia with failed reflow. J Pathol 78:105–120
40. Stahl RAK, Thaiss F, Kahf S, Schoeppe W, Helmchen UM (1990) Immune-mediated mesangial cell injury – Biosynthesis and function of prostanoids. Kidney Int 38:273–281
41. Suzuki Y, Churg J, Grishman E, Mautner W, Dachs S (1963) The mesangium of the renal glomerulus: Electron microscopic studies of pathologic alterations. Am J Pathol 43:555–578
42. Tuttle SE, Sharma HM, Bay WH, Heybert LH (1985) Glomerular basement membrane splitting and microaneurysm formation associated with nitrosourea therapy. Am J Nephrol 5:388–394
43. Yajima G (1976) A histopathological study on diabetic nephropathy – light and electron microscopic observations. Acta Pathol Jpn 26:47-62
44. Yamamoto T, Wilson CB (1987) Quantitative and qualitative studies of antibody-induced mesangial cell damage in the rat. Kidney Int 32:514–525